SURFACE MODIFICATION OF 6H-SiC UNDER VACUUM ANNEALING STUDIED BY TIME OF FLIGHT POSITRON ANNIHILATION INDUCED AUGER ELECTRON SPECTROSCOPY

by

SAURABH MUKHERJEE

Presented to the Faculty of the Graduate School of

The University of Texas at Arlington in Partial Fulfillment

Of the Requirements

for the Degree of

MASTER OF SCIENCE IN MATERIALS SCIENCE AND ENGINEERING

THE UNIVERSITY OF TEXAS AT ARLINGTON

May 2007

ACKNOWLEDGEMENTS

Writing this thesis has given me a great opportunity to work closely with some of very inspiring people. They have always been around to give me encouragement and see me through the blues.

My immense gratitude to Dr. Alex Weiss who agreed to teach me the nuances of experimental physics and Materials Science and is my supervisor for the thesis. He was always there to encourage me and give me advice regarding everything from science to general life.I would also like to take this chance to thank Dr. Aswath, Dr. Priya, Dr. Hao, Dr. Meletis and Dr. Fry who have always helped me in making the right decision and sharpen my basics. My special thanks to Dr. Gerhard Brauer of INSTITUT FOR IONENSTRAHLPHYSIK UND MATERIALFORSCHUNG, FORSCHUNGSZENTRUM , Germany who supplied us with the 6H-SiC sample .My sincere regards to Manori who taught me a lot about the positrons and for making the work in the lab look like fun. Thanks to Brian who taught me things which one would normally not find in textbook. I would like to thank other group members like Raji, Ameena for their initial help. Doug is another person who has helped immensely. He was always there with his usual words of encouragement to help me when anything broke down.

My deepest regard to my family members for supporting me through thick and thin.

December 18, 2006

ABSTRACT

STUDY OF 6H-SiC AND POLYCRYSTAL GOLD SURFACES USING TIME-OF-FLIGHT POSITRON INDUCED AUGER ELECTRON SPECTROSCOPY

Publication no._____

Saurabh Mukherjee, MS

The University of Texas at Arlington, 2006

Supervising Professor: Alex .H. Weiss

This thesis presents the first study of vacuum annealing of 6H- SiC surface using Time-of-Flight-Positron Annihilation induced Auger Electron Spectroscopy(TOF-PAES) . The study was the first application of a TOF-PAES spectrometer to the SiC. The increased efficiency of the TOF-PAES allows us to see simultaneously for the first time Si-LVV, C-KVV, O-KVV peaks in the PAES spectrum for SiC. The top layer surface concentrations of C, O and Si were monitored by TOF-PAES surface. The results indicate that the SiC surface was initially covered with a layer containing oxygen but largely devoid of Si which was subsequently removed as a result of vacuum annealing to expose Si and C in the top layer. These results clearly demonstrate the utility of PAES in

the study of the surface modification of SiC. In addition, the reduced secondary background associated with PAES made it possible to observe, for the first time, low energy Auger transitions from SiC at 37eV, and 53 eV. In order to confirm the reliability and efficiency of the T-O-F PAES spectrometer in measuring Auger peaks at such low energies, TOF-PAES was used to measure previously observed low energy Auger transitions in Au. The increased efficiency of the T-O-F PAES permitted us to make the first measurement of the individual low energy peaks (37ev, 56eV, 71 eV) in Au demonstrated the sensitivity of the spectrometer to the low energy auger electrons. This data was used to make the first experimental estimates of the relative annihilation probabilities of positron with 5d, 4f, and 5s core electrons which when compared with the theoretical values reveal a partial failure of the theory to account for the relative annihilation probabilities of electrons in the 5s level.

TABLE OF CONTENTS

LIST OF ILLUSTRATIONS

Figure Page

LIST OF TABLES

Table Page

CHAPTER 1

INTRODUCTION

1.1 Overview

Silicon Carbide is a wide band gap semiconductor whose high thermal conductivity and fast free carrier recombination[1] give it great potential utility in high temperature and high frequency applications. It exists in monocrystalline , hexagonal polytype form, the most common being 6H-SiC and 4H-SiC.The different polytypes offer a wide range of the band gaps with very little lattice mismatch. SiC and its composites have found wide application as materials for automobile engines, fuel cell/turbine hybrid system, nuclear fusion reactors.[2] This thesis reports experimental research in which Time-of-Flight Positron Annihilation induced Auger Electron Spectroscopy (TOF-PAES) has been used to study surface changes due to vacuum annealing of 6H- SiC The results of these studies demonstrate the ability of PAES to probe the low energy portion of the Auger electron spectrum of SiC. In the course of this research low energy Auger peaks not reported previously were observed in the PAES spectrum from SiC. In order to demonstrate the reliability and sensitivity of the TOF-PAES, (which up till now has been used to study higher energy Auger transitions) to low energy Auger peaks), measurements were performed of known low energy Auger peaks of Au. The increased efficiency of the T-O-F PAES permitted us to make the first measurement of the individual low energy peaks (at 37ev, 56eV and 71 eV) in Au demonstrated the sensitivity of the spectrometer to the low energy Auger electrons. This

data was used to make the first experimental estimates of the relative annihilation probabilities of positron with 5d, 4f, and 5s core electrons which when compared with the theoretical values reveal a partial failure of the theory to account for the relative annihilation probabilities of electrons in the 5s level.

1.2 Positron Trapping

Positron is theantiparticle of electron having the same mass, spin but a charge of +e rather then –e. It was first postulated by P.A.M. Dirac in 1929[3] and discovered by C. Anderson in 1932.[4] Positron Spectroscopies used in the characterization of materials are- Positron Lifetime spectroscopy, Doppler Broadening gamma Spectroscopy, Angular correlation of Annihilation Radiation (ACAR), Positron Induced Auger Electron Spectroscopy. The first two methods are used to study the open volume defects in materials while ACAR is used to study the electronic structure of the materials. More recently Positron Spectroscopies including PAES have been developed for the study of surfaces. In order to understand these techniques it is important to understand the interaction of Positron with the surfaces.

When a positron is incident on a surface a number of important events take place- Positron Reemission, Positronium formation and emission and the trapping of positron in surface state. The positron interaction with surface is illustrated in fig 1.1. Positrons loose energy via elastic interaction with the surface atoms, core electron excitation and secondary electron formation as shown in 1.1(a). A few percent elastically scatter from the outermost atomic layer giving rise to Low Energy positron Diffraction (LEPD). Fig 1.1 (b) shows positron penetrating inside the surface and loosing energy via electron – hole pair production and phonons. Positrons can also pick up an electron and form non-

thermalized Positronium or be reemitted as a free positrons (the signal relevant to Positron Reemission spectroscopy) before attaining thermal equilibrium. An important process for this study is the thermalized positrons getting trapped in an image correlation well at the surface and annihilate with the electrons emitting 2 gamma rays of 511keV energy. These trapped positrons can form positronium and be emitted in vacuum. A few percent of the trapped positrons annihilate with the core electrons of the surface atoms (~5%) and emit the two back to back gamma rays of 511 keV energy. This process is rapidly (within~10^{-14}sec) followed by the emission of the Auger Electron.

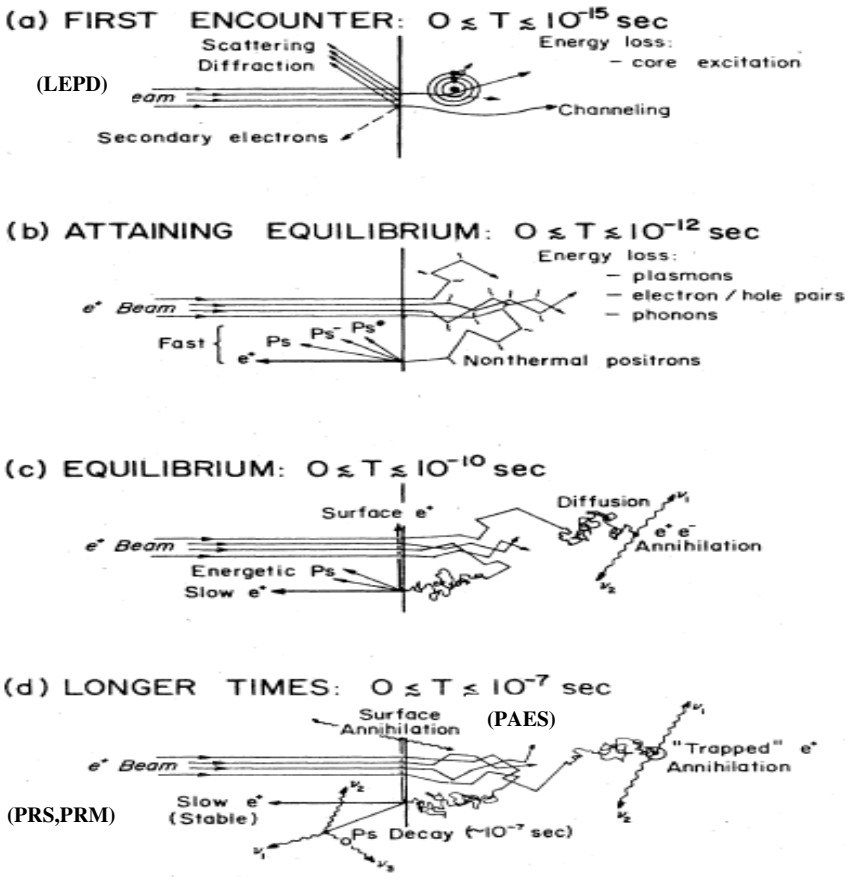

Figure 1.1: The Interaction of positron beam (E ≤ 100keV) with the near-surface region of a solid [5]

1.3 Introduction to Positron Induced Auger Electron Spectroscopy

Conventional method of Auger Electron Spectroscopy makes use of an energetic beam of electron or photons to knock out core electrons. The atom then rearranges by emitting an Auger electron. In Electron Induced Auger Electron Spectroscopy (EAES), high energy electrons (>1KeV) knock out the core electron. Fig1.2 shows the energy level diagram and the transitions involved in EAES. The energetic electron hits the core level electron (K-shell) and knocks it out. The other tightly bound electron (L_1-shell) fill the resultant hole. The extra energy now available to the atom is transferred to the other electron (L_2-shell) which escapes as an Auger electron. The nomenclature of an Auger transition is based on the three shells involved in the Auger Process, like the one in fig1.3 the Auger electron is the result of "KL_1L_2" transition. Hence the kinetic Energy of the Auger electron is given by

$$E_{KL_1L_2} = E_K - E_{L_1} - E_{L_2'} - \phi$$

Where E_K E_{L_1} $E_{L_2'}$ is the binding energy of electrons in the K, L_1, L_2 levels respectively. ϕ is the work function of the surface. $E_{L_2'}$ is different from E_{L_2} due to Coulomb interaction between the two holes in the final state. EAES is limited in its application due to the higher depth of excitation of the energetic electron probe. Since the core-holes are created by electron impact ,the incident electron beam must have an energy in excess of the binding energy of the core-hole. Typically electron beam energies of 3 to 5 KeV is used .Electrons with kilovolt of energies excite auger transitions thousands of angstrom below the surface. However Auger electrons from layers deeper then a few nanometers

have a high probability of losing energy on their way out of the sample and become part of an inelastic tail. Electrons in the EAES peaks represent those which came from near the surface and have not lost energy.

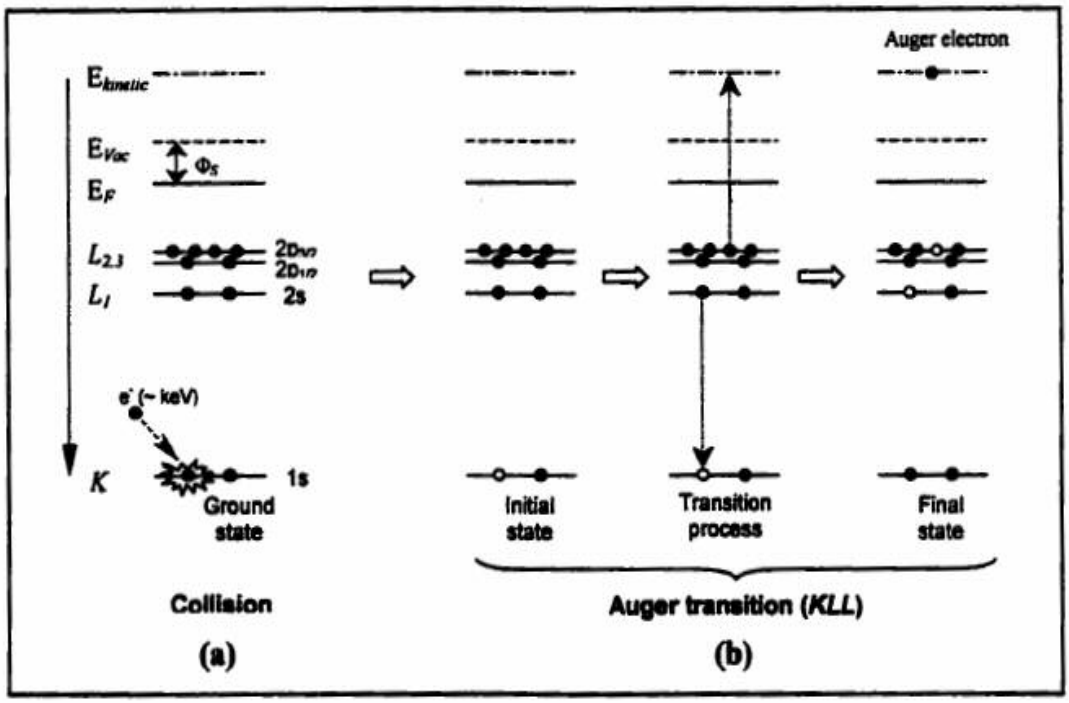

Figure 1.2 Electron induced Auger electron process with energy diagram

1.3.1 POSITRON induced AUGER ELECTRON SPECTROSCOPY

A similar mechanism applies for Positron induced Auger Electron Spectroscopy (PAES). The difference here is that the core hole is created by positron-electron annihilation[7,8] and hence the energy of the incident positrons can be made very low(<25eV).. Fig1.5 shows the PAES mechanism. The slow positrons are incident on the material. They are slowed down by various inelastic processes and diffuse back to the surface and get trapped in the surface state with high efficiency. A few percent of the

positrons in the surface state annihilate with the core electrons resulting in core-hole excitation that will typically be followed by Auger electron emission. Since the surface state positrons are highly localized in the direction normal to the surface, almost all the annihilations of surface state positrons are with atoms in the topmost atomic layer. Thus the PAES signal is representative of atoms at the topmost layer.

In the PAES the core-holes are created by matter –antimatter annihilation thus it is possible to use an incident beam energy below that of the Auger electron and eliminate the large secondary electron background present in EAES. Secondary electrons produced by the collision of positron with the electrons cannot have energy larger then the kinetic energy of the incident positrons.

$$KE_{\text{sec}} \leq E_p - \phi^+ + \phi^-$$

Where KE_{sec} is the kinetic energy of the secondary electrons as they leave the surface, E_p is the incident positron energy and ϕ^+ and ϕ^- are the work function of positron and electron respectively. If E_p is made smaller then the Kinetic energy of the Auger Electron, the secondary electron background under the Auger peak is largely reduced.

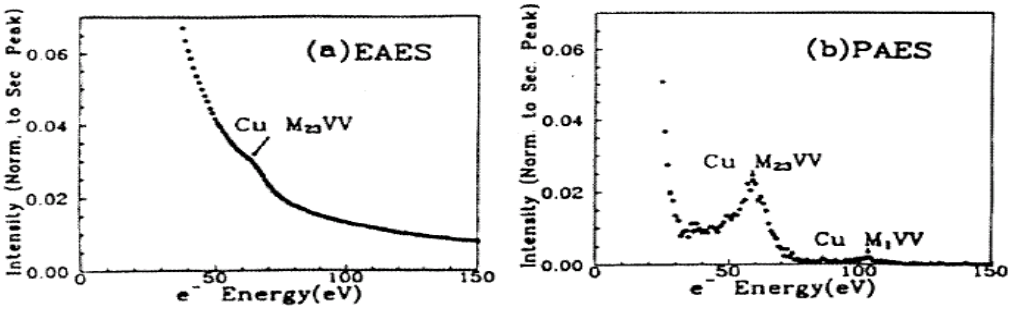

Figure 1.3 Comparison of PAES and EAES spectrum from Cu (110) surface[7]

The PAES mechanism was first demonstrated in 1987 [8] by A.H. Weiss. It has been shown that PAES can be used to eliminate the secondary electron background and that the PAES signal originates from the annihilation of the positrons in surface state resulting in PAES probing the topmost atomic layer. Early theoretical work was carried out by Jensen and Weiss[9] and subsequently extended by Fazleev, Fry and coworkers.[10] Applications of PAES have been extended to study the surface of metals, semiconductor and oxide surfaces.[11-13]

1.3.2 Surface Sensitivity of PAES

The enhanced surface sensitivity of PAES stems from the positron trapping effect as mentioned before , which has been proved by a series of measurements performed on single crystal Cu with varying coverage of S. [14] Low energy positrons implanted into a metal or semiconductor have a high probability of diffusing back to the surface and becoming trapped in an "image correlation well" before they annihilate.[15] The trapped positrons are localized and annihilate almost exclusively with the atoms at the surface. This enables PAES to have a probe depth of approximately 1-3 Å. In contrast, conventional Auger techniques, the probe depth is from 4-20 Å depending on the energy of Auger electron peak. The probe depth is set by the escape depth of the Auger electron. Fig 1.5 is a comparison of the mechanism leading to surface selectivity in PAES and EAES.

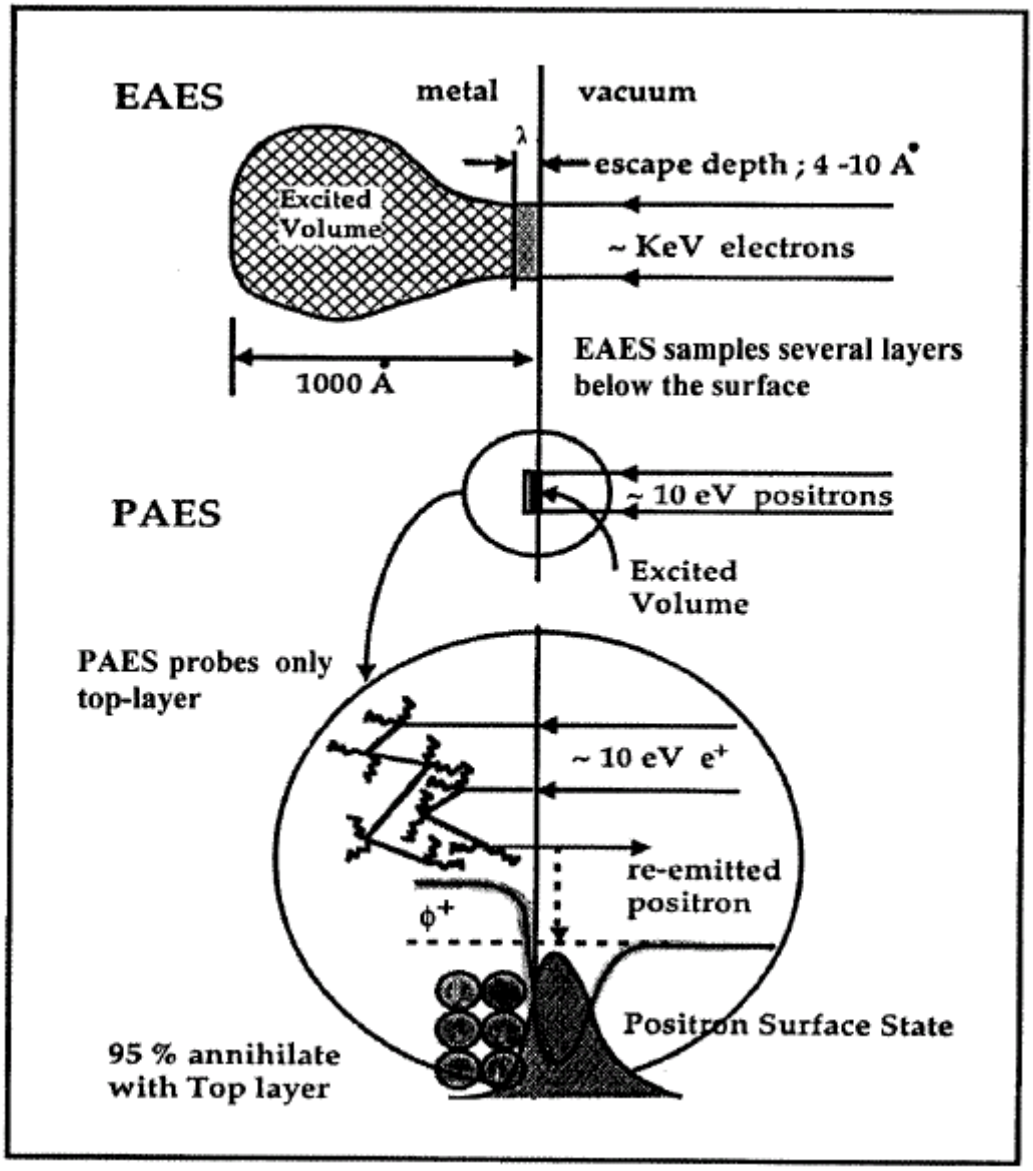

Figure 1.4 Comparison of surface selectivity in PAES and EAES[16]

First principal methods for calculating PAES intensities, positron surface states and positron work function have been developed by Fazleev et al.[17-18]. Fig 1.6 shows the Cu (100) surface potential and the ground state wave function of the positron.[19] Fig 6(a) is the potential seen by a positron on Cu (100) surface. It shows a minimum potential just

outside the surface, where most positrons diffusing from the bulk will be trapped, fig1.6 (b) is the wave function of the trapped positrons. The wave function has an appreciable value over the area outside the surface and on the first layer. The probability of finding a positron below the first layer is typically only a few percent. As a consequence , almost all the positron annihilation will happen on the surface and almost all Auger signal comes from the top first layer(~95% for the Cu (100) surface).

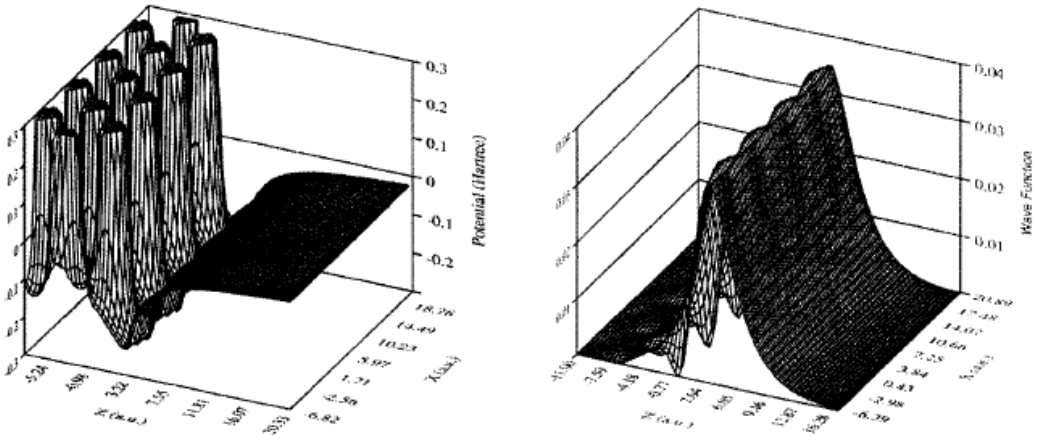

Figure 1.5 Positron surface states. (a) Positron potential and (b) positron wave function on the Cu (100) surface[20]

1.3.3 Time of Flight Technique

Time –of- Flight (TOF) technique is a method to measure the kinetic energy of a particle by measuring its speed, which can be determined by the time it takes to travel a fixed distance. Positron experiments have been benefited from the advantage of the time-of –flight method over the past twenty –five years. The first laboratory based positron

beam measurements of scattering in gases were the TOF measurement at University College, London.[22] Suzuki and his coworkers first utilized the TOF technique in positron annihilation induced Auger Spectroscopy research in 1995.[23] They developed an apparatus for PAES with the Time –of- Flight (TOF) technique using a short pulsed slow positron beam. High –count rate measurement (~10 min/spectrum) was carried out by the use of an intense slow positron beam (~108 e^+/s) generated with an electron linear accelerator (LINAC).But their spectrum has a large background which led to poor resolution. The Time-of –Flight Spectrometer used in our laboratory uses an innovative timing method suitable to our magnetically guided DC positron beam system.[21] High resolution spectra are obtained by as much as a factor of 100 times as compared to our conventional PAES system that utilizes sequentially scanned energy analyzer, such as CMA.[20]

The first TOF- PAES system using a DC beam was considered at UTA. In the UTA TOF- PAES system the flight time of the Auger electron is determined by the time interval between the detection of the γ-ray signal emitted from the positron –electron annihilation and the signal from the detection of an Auger electron. When an electron with energy E travels a fixed distance λ at a velocity ν through an electric field free region, "the time of flight" may be found by using

$$t = \frac{L}{v} = \sqrt{\frac{m_e}{2E}} \cdot L \qquad \text{Eq (1.1)}$$

Where m_e, E, v are the mass of the electron, the electron Kinetic Energy and the speed of electron respectively.

The reason for the high efficiency of TOF-PAES is the parallel acquisition of electron signal. In conventional techniques, the Auger spectrum is obtained by scanning a narrow energy window. Consequently only a small fraction of the spectra is detected and much useful signal is wasted. But in the TOF technique, electrons with all energies in the spectra are accepted and sorted. This leads to an increase in efficiency for the TOF system which can be estimated by:

$$\frac{\varepsilon_{TOF}}{\varepsilon_{Conv}} = \frac{E_{\max} - E_{\min}}{\Delta E_{analyzer}} \qquad \text{Eq. (1.2)}^{21}$$

Where $\frac{\varepsilon_{TOF}}{\varepsilon_{Conv}}$ is the ratio of the TOF efficiency to that of the conventional spectrometer .

CHAPTER 2

EXPERIMENTAL SETUP

The system used for the experiment here was Time of Flight – Positron Annihilation Induced Auger Electron Spectroscopy (TOF-PAES). TOF-PAES consists of –magnetically guided positron beam, UHV system, detection system, sample preparation and transfer chamber. TOF –PAES was developed in UTA and has faster data acquisition and increased resolution then the earlier PAES system. The earlier PAES apparatus was fitted with a CMA analyzer where data was acquired sequentially. Earlier PAES studies with SiC haven't revealed the existence of Carbon and Oxygen on the surface and hence the variation in C signal intensity couldn't be monitored. TOF-PAES allows for parallel data acquisition and at a faster rate letting us to monitor the surface concentration of Si, C, and O with different annealing temperatures.

2.1 UHV system

The system used here is 5.4 m long and 1.8 m wide. It is made up of radioactive source chamber, magnetic guided beam line, Micro channel plate, Time of flight tube, sample preparation chamber, gas lines and vacuum pumps. Radioactive Source area is located on the right side of the Fig2.2 and a gate valve - V1 (MDC GV 1500M) separates it from the rest of the system. Sample preparation chamber is located on the left side of Fig 2.2 and is isolated by another gate valve- V2 (MDC). As shown in fig.2.3 Gate Valve (V3) separates the Sample Preparation chamber to the Turbo Pump. The gate valves are

used to isolate the radioactive source area to the atmosphere while the sample is being changed. They also help in isolating the MCP from exposure to the atmosphere and decrease the sample changing time.

The details of the Vacuum Pumps are given in table 2.1. With the aid of these pumps, the chamber can be pumped down below 6×10^{-10} Torr. The Turbo pump is equipped with a N_2 leak valve which is used to vent the chamber and change the sample. The evacuation of the chamber is made initially by the mechanical pump to 30milliTorr. The turbo pump is then started and used to pump the chamber down to 2×10^{-6} Torr. Baking of the chamber is started at this pressure and is accomplished by the heating tapes which raise the temperature to 100-120^{o}C and the system is maintained at this temperature for 24 hrs. After this the pressure is in 10^{-8} Torr. Then the Ion Pump valve is opened and the chamber is allowed to be pumped by the Ion Pump for 12 hrs while the Turbo pump is switched off. After this the baking is stopped and the chamber is allowed to cool down. After the cooling down the final pressure achieved is in the range of 6×10^{-10} Torr.

2.2 Low Energy Positron Production

The positron source used in TOF-PAES is Na-22 (NER-407) source, which was bought from NEN-Du Pont Company. Initially it had activity of 100mCi and 4.08mCi at the time of run of the experiment. Na-22 has half life of 2.6 years and hence the flux of positrons can be considered to be constant during the run of experiment which is normally for several days. Currently, the generation rate of positron is about 1.509×10^{8} per sec.

The nuclear reaction occurring during decay of Na-22 is-

$$^{22}_{11}Na \xrightarrow{\beta^+} {}^{22}_{10}Ne + \beta^+ + \upsilon \qquad \text{Eq. (2.1)}$$

Where β^+ is a positron and υ is a neutrino. The positrons emitted from Na-22 have a wide energy distribution.[20] These positrons are not fit to be used as probe for TOF-PAES. A moderator is used to moderate the positrons. As the high energy positrons implant in the moderator they rapidly thermalize and are slowed down. Some of them annihilate inside the moderator bulk while some diffuse to the other surface and are trapped in the surface states. These positron can be reemitted or escape as positronium. The reemitted positrons escape with energy $E = |\Phi +|$ where $\Phi +$ is the work function of the material. Moderators have negative work function so that the positrons can be reemitted spontaneously. Our system uses a transmission type polycrystalline moderator. It is 1μm thick, 9mm diameter foil supplied by AARHUS University, Denmark. It was annealed to 2000^{o}C by electron beam heating and its efficiency is ~ 10^{-4}.

The slow positrons emitted are mixed with gamma rays and high energy positrons which need to be filtered out. The positron transport system [20] filters out the fast positrons and the gamma rays and is used to control the incident beam energy.

The transport system has five parts: the fast positron and γ rays filter, the positron accelerator, an incident /secondary beam separator, time-of-flight retarding tube and a system of coils and permanent magnets to establish the appropriate magnetic field. The transverse magnetic field generated by two sets of rectangular Helmholtz frames to compensate for the earth's magnetic field. One set is used for the source region and other is for the target region. A series of short solenoidal coils is used to establish an axial

magnetic field to guide the positron beam to the sample direction.[20] A positron with a velocity vector at some angle to the magnetic field will follow a spiral trajectory along the magnetic field lines. A total of 20 solenoid coils were used to produce the axial magnetic field.[20] The energy filter used to filter out high energy positrons and the gamma ray work as follows. A positron moving in the crossed electric and magnetic field travels along a complex spiral trajectory as shown in Fig 2.4[20]

After passing through the $\vec{E} \times \vec{B}$ region, the positron is displaced from its original trajectory in the $\vec{E} \times \vec{B}$ region according to the equation:

$$y = \frac{E \cdot L}{2B} \sqrt{\frac{m_p}{2E_k}} \qquad \text{Eq (2.2)}^{20}$$

Where E_k is the positron kinetic energy before deflection, m_p is the mass of the positron, E is the magnitude of the electric field, B is the magnitude of the magnetic field and L is the length of the electric field. Accordingly, only those positrons with appropriate energy can pass through the hole in the tungsten barrier C, which is 5/8 inch offset from the central axis. All other positrons and γ rays are blocked by the tungsten barrier C[20]. The fast positrons and γ rays filter are shown to the left side of the radioactive source and the moderator in fig 2.1. The filter consists of tungsten barriers B and C and $\vec{E} \times \vec{B}$ plates A and B. The γ rays are not affected by the electrical or the magnetic fields and are stopped by the tungsten barrier C. The fast positrons are only minimally deflected and hence are also stopped by the tungsten barrier C. The positron accelerator is mounted between the sets $\vec{E} \times \vec{B}$ plates labeled B and C. It is used to provide a uniform axial electric field to accelerate the positrons to a specified energy.

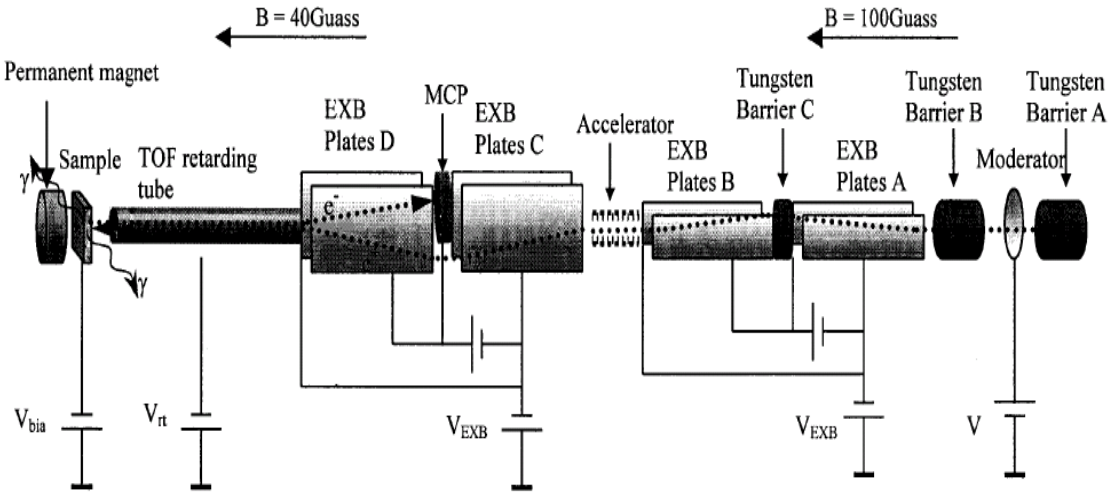

Figure 2.1. Slow Positron beam transport system in TOF-PAES [20]

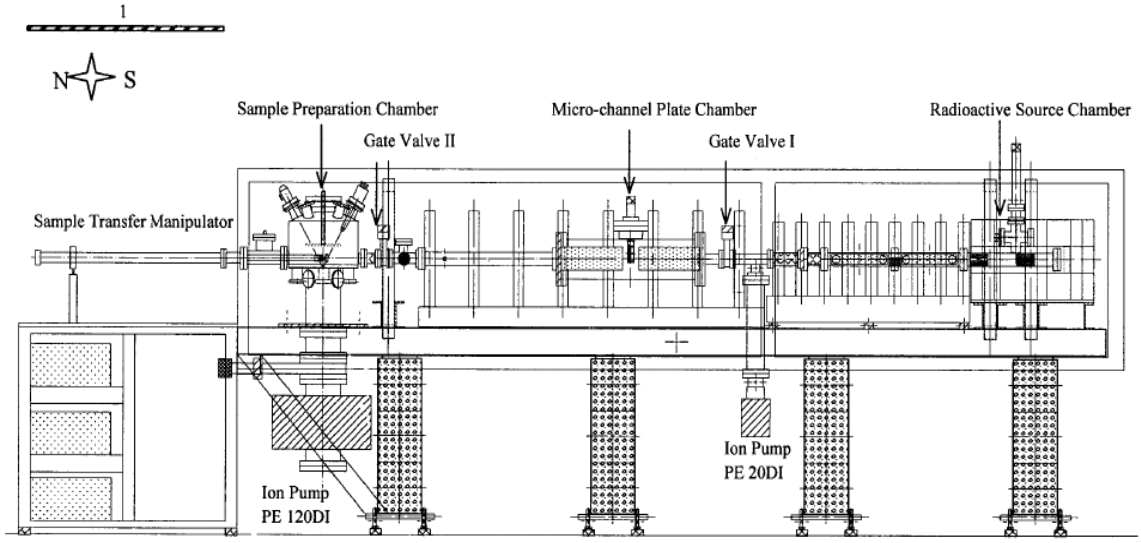

Figure 2.2. A schematic diagram of TOF-PAES instrument and the UHV system[20]

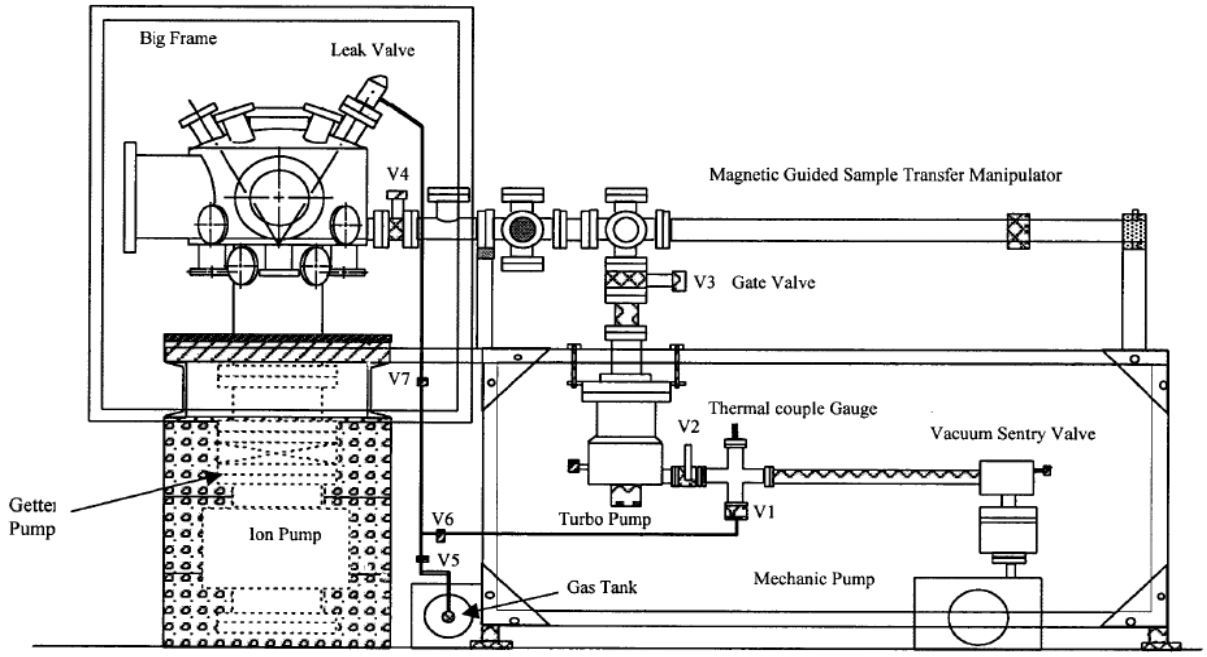

Figure 2.3 A schematic diagram of Sample preparation chamber and vacuum pumps [20]

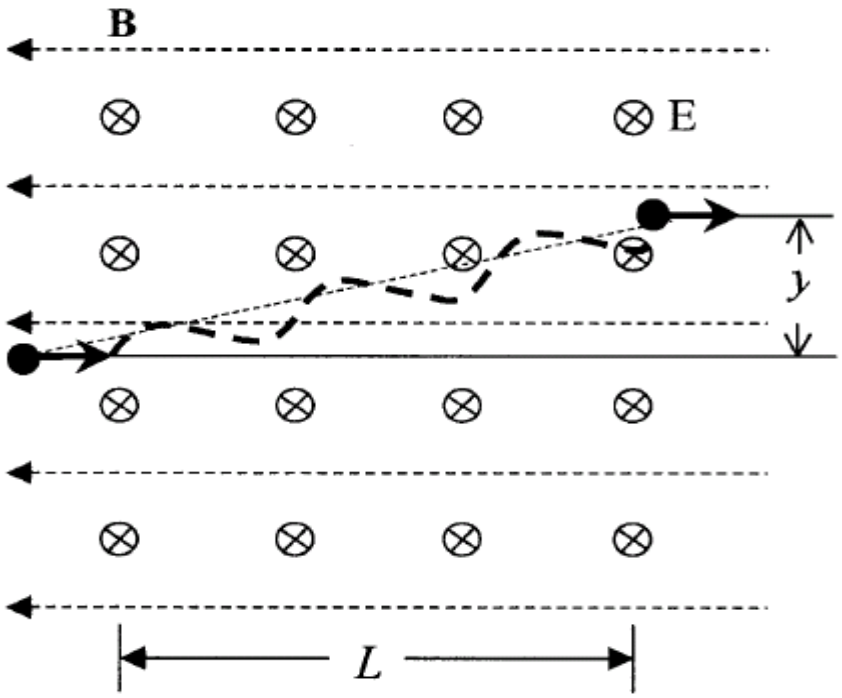

Figure 2.4 Positron trajectory in the electromagnetic field[20]

Another two sets of $\vec{E} \times \vec{B}$ plates are used to deflect the incident beam around the MCP and to separate the incident slow positron beam from the electrons emitted from the sample. The positron beam is deflected downward by $\vec{E} \times \vec{B}$ plates C and upward by $\vec{E} \times \vec{B}$ plates D to get around the MCP. Auger and secondary electrons from the target will be deflected to the MCP detector by $\vec{E} \times \vec{B}$ plates D.

The time-of-flight retarding tube(TOF tube) is used to establish a retarding potential in the vacuum tube. The electrons emitted by the target are slowed down when they enter the TOF tube but return back to their original energy as they travel between the TOF tube and the MCP. So by adjusting the TOF tube bias we can stop low energy impact induced secondary electrons from reaching the MCP. This can improve the Auger signal quality significantly by eliminating background due to events that can mimic the

Auger signal in which an impact induced secondary electron arrives shortly after the delayed gamma ray signal is detected by the BaF_2 which happens to come from the annihilation of the positronium. Maximum voltage applicable to the TOF tube is -1000 V. Normally the bias is set just above the maximum energy of the secondary electrons induced by the positron beam i.e. ~2eV above the normal positron beam energy.

2.3 Detection system

There are two kind of signal sources present during the PAES measurement: charged particle (electron and positrons) and electromagnetic waves (such as γ rays). γ rays are created by positron-electron annihilation and other electromagnetic waves come from excited atom relaxation, γ rays scattering and charged particle deceleration. Electrons are produced by positron bombardment, Auger process, electromagnetic wave excitation and electron collision. There are also some charged particles and electromagnetic waves coming from the background environment. Useful signal are γ rays and Auger electrons. Other signals constitute background and it is desirable to eliminate them from the PAES measurement.

In the TOF-PAES system, γ rays are detected using a Barium Fluoride (BaF_2) detector and a Sodium Iodide (NaI) detector.[20] The BaF_2 detector was purchased from REXON Componenets, Inc. To protect the BaF_2 detector from the magnetic fields, it is shielded by two concentric magnetic shields, the inner shield being a Co-Netic alloy 25P70 cylinder and the outer shield being a Netic s3-6 high saturation alloy cylinder, both purchased from magnetic Shield Corp.[20]

The pulse generated by the BaF_2 detector is proportional to the incident gamma ray energy. The falling edge of the negative pulse from the BaF_2 detector is used to

trigger the timing electronics.[20] Fall time is about 1.8 ns which is much smaller then the Auger electron travel time from sample to the multi channel plate which is estimated to be 100ns. The CFD can determine the time of the pulse with an accuracy that is considerably less than the fall time. Consequently the timing resolution of the BaF_2 detector is less than 1ns.

A micro channel plate (MCP) is used to detect electron emitted from the sample surface. MCP is a two-dimensional array of 10^4-10^7 short single channel electron multipliers whose sizes are in the range of micrometers.[20] The MCP was made by Burle Company. A typical pulse from MCP has a falling edge of about 1.8 ns.[20] This makes the MCP a good timing detector for Auger electron flight time measurement.

2.4 Time of Flight data Acquisition system

The time-of-flight data acquisition system is the core part of the TOF-PAES system. It measures the flight time of an electron from which its energy is calculated. When a positron annihilates with an electron, typically two or three γ rays will be emitted. The short time interval between annihilation and Auger electron emission (only ~10^{-14} seconds) makes it feasible to use the γ ray signal as the start time of the Auger electron flight time as the electrons take normally 100 to 1000 ns to reach the MCP and provide the stop signal. In the typical configuration the γ ray signal is delayed by 700 ns-2000ns and set to be stop signal while the electron signal from MCP is set to be start signal. This time interval Δt can be measured by TAC and used to calculate the electron kinetic energy using $E = \frac{1}{2}mv^2 \propto (\frac{L}{\Delta t})^2$. The MCP pulse was chosen as the start signal

because the MCP count rate is ~10 times smaller then the BaF_2 signal. After receiving one start signal until it receives a stop signal or until it receives the end of its range.[20]

Once the flight time is determined, a signal is sent to computer memory to form the TOF-PAES spectrum. An EG&G Ortec ADCAM advanced data collection and management system is used to monitor the experimental data acquisition process. The flight time is processed by a TRUMP/2K multichannel analyzer (MCA) card, which is controlled by the software package MAESTRO.

2.5 Sample Preparation System

The sample preparation system is located in the sample preparation chamber. It consists of a sample holder, a sample transfer manipulator, a sputtering gun, gas lines and a Low Energy Electron Diffraction (LEED) system (as shown in the Fig 2.12)

The sample preparation chamber is a custom made by MDC Inc. It consists of a stainless steel cylinder 12 inches in diameter and 14 inches high with 28 access ports. A Perkin Elmer sputtering gun (model 104-191) is mounted on the chamber through a 2.75 inches port. Its control unit is model PHI 20-115. Gas lines which are used to provide sputtering gases (such as Ar and Ne) or controlled gas environment are connected with sample preparation chamber with a Varian variable leak valve(model 951-5100) through another 2.75 port. Sample transfer is realized by a linear feed-through (MDC 954-5151) to move the sample from preparation chamber to TOF analysis positron. One UHV current feed-through is mounted on the chamber for admitting power for the button heater.

The sample holder is made from non-magnetic stainless steel and mounted on the linear transfer manipulator. It is isolated from the manipulator and the sample may be

biased up to ± 1000 V through a UHV feedthrough. The sample holder is designed to hold a sample with a maximum size of 1.2 inches in diameter. A permanent magnet disk (1 inch in diameter and ¼ inches thick) imbedded in the sample holder provides a strong divergent magnetic field around the sample. Magnetic field decreases rapidly as the distance from the sample surface increases (as shown in fig 2.7).

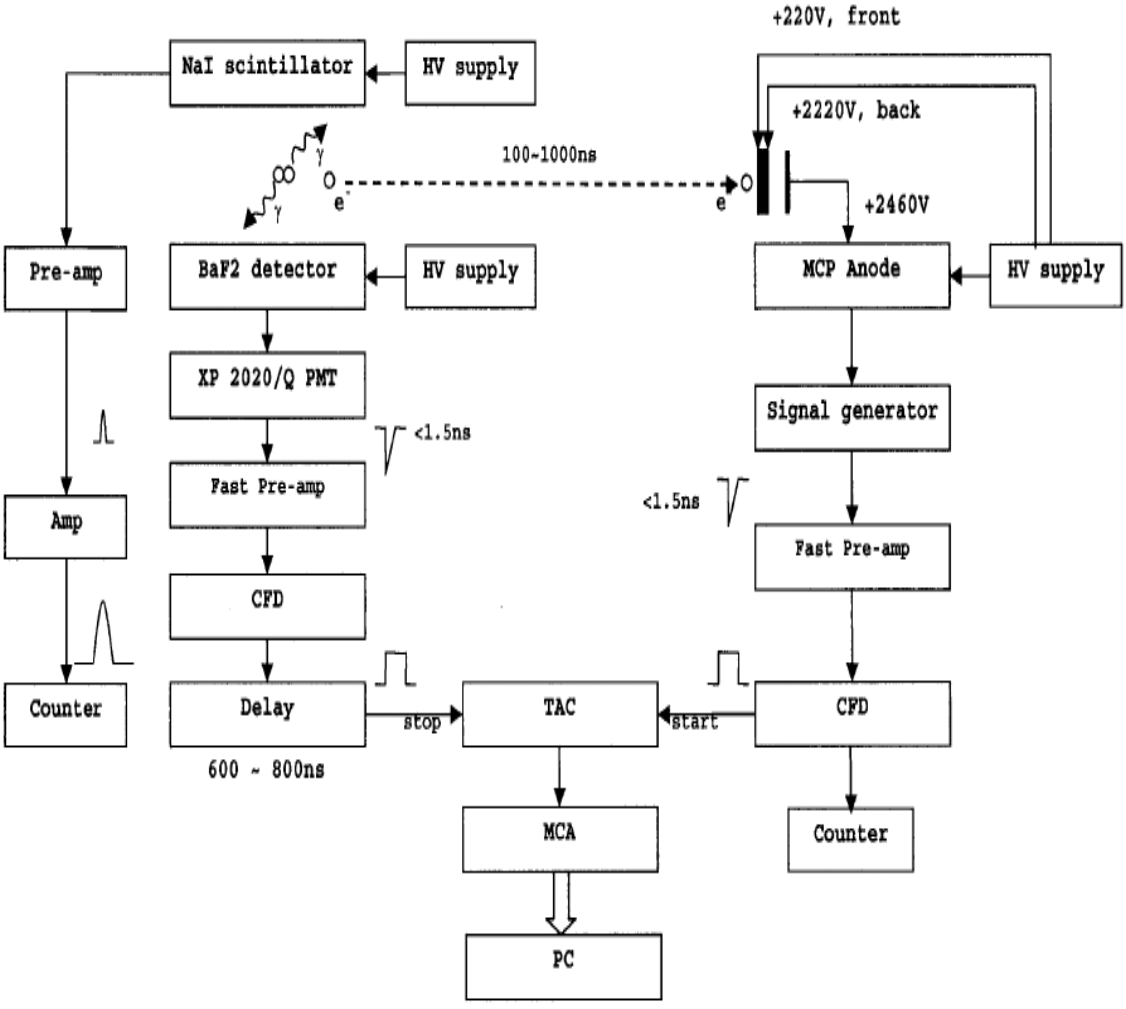

Figure 2.5 Time of Flight data acquisition system[20]

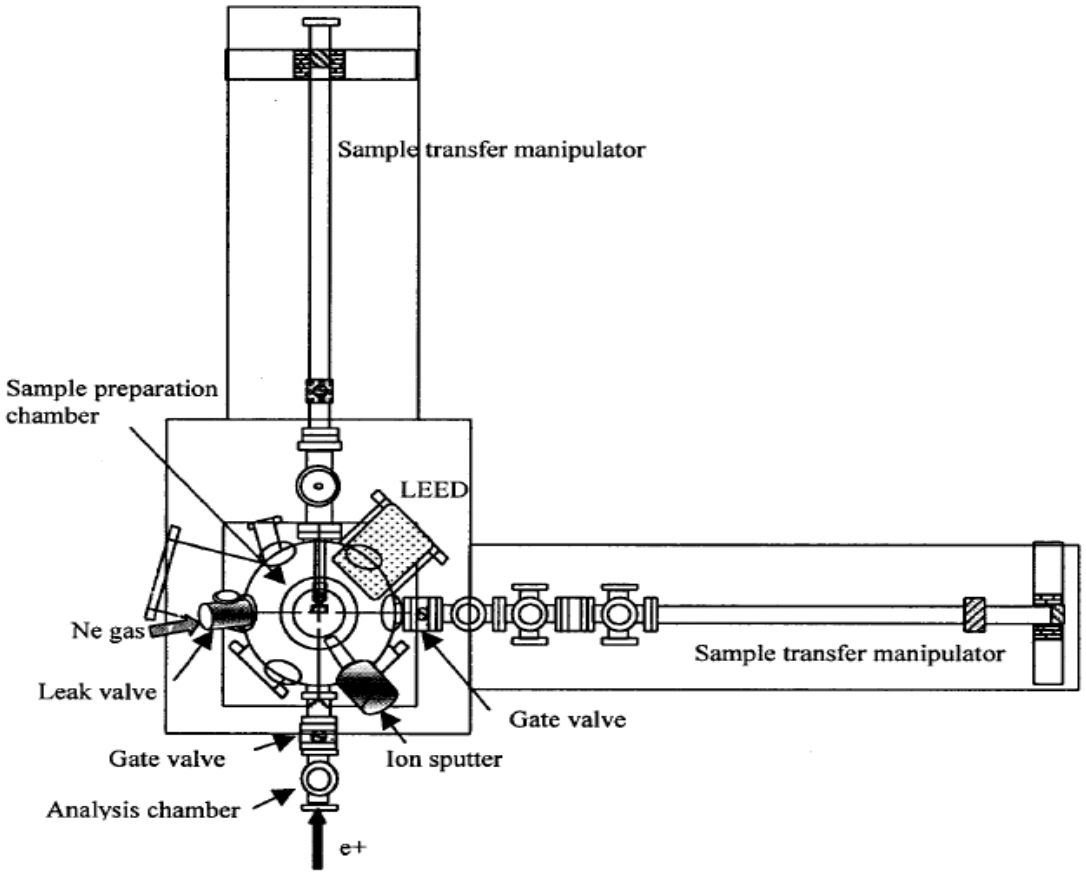

Figure 2.6 Top view of the Sample preparation chamber [20]

This divergent field serves to parallelize the trajectory of electrons emitted from the sample surface and increase the efficiency of data acquisition. The principal is illustrated in fig 2.7.

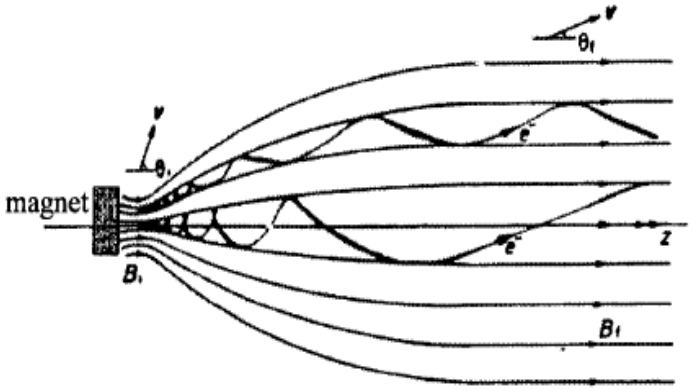

Figure 2.7 Illustration of the parallelization mechanism by divergent magnetic field[20]

Samples used in this experiment were 6H- SiC epitaxial layers grown on a Si(100) substrate (from CREE Inc.). The Au foil was bought from Alfa Aesar (99.998% purity, 0.001 inches thick , 1inchX1 inch). Both the sample was placed in the PAES chamber with no chemical pretreatment. The chamber was pumped down to $1X10^{-8}$ Torr. The chamber was left unbaked in order to avoid thermal modification of the surface before measurement

CHAPTER 3

RESULT AND DISCUSSION

3.1 6H-SiC annealing results

Figure 3.1.1 shows the calibration curve for 6H-SiC. We measure the channel number of secondary electron peak change with sample bias. Since the corresponding energy value of each peak is equal the sample potential plus 2~3 eV, we get the relationship of secondary peak with its energy. According to relationship of channel number ($\#_r$) with E, we use the following function to fit the data points and obtain the parameters for the function.

$$\#_r = P_1 - \frac{P_2}{\sqrt{E}} \qquad \text{Eq (3.1)}^{20}$$

P_1 and P_2 are the constants to be determined by curve fitting. If the TOF retarding tube is under negative bias, it will slow down the electrons when they enter the tube. This effect is taken into account using the following function:

$$\#_r = P_1 - \frac{P_2}{\sqrt{E - P_3}} \qquad \text{Eq (3.2)}^{20}$$

Where P_1 is proportional to the delay and P_3 accounts for the TOF bias. The energy spectrum can be calculated from channel spectrum after the parameters P_1, P_2 and P_3 are found by fitting the calibration curve :

$$N(\#_r)\left(\frac{(P_1 - \#_r)^3}{2P_2^2}\right) \rightarrow N'(\#_r) \xrightarrow{E = \frac{P_2^2}{(\#_r - P_1)^2} + P_3} N(E)$$

For 6H-SiC sample, the incident positron beam energy is 15eV, sample is biased at -20V, the TOF retarding tube is applied -17V, Delay time is 700ns and TAC range is 800ns. The energy of secondary electron peak with its corresponding channel number is shown in figure 3.1. By fitting the data points with Eq. 3.1, we obtained a very good result as shown in the figure 3.1.1, and the conversion function is:

$$\#_r = 1714.13164 - \frac{3623.43995}{\sqrt{E - 11.40508}} \qquad \text{Eq(3.3)}$$

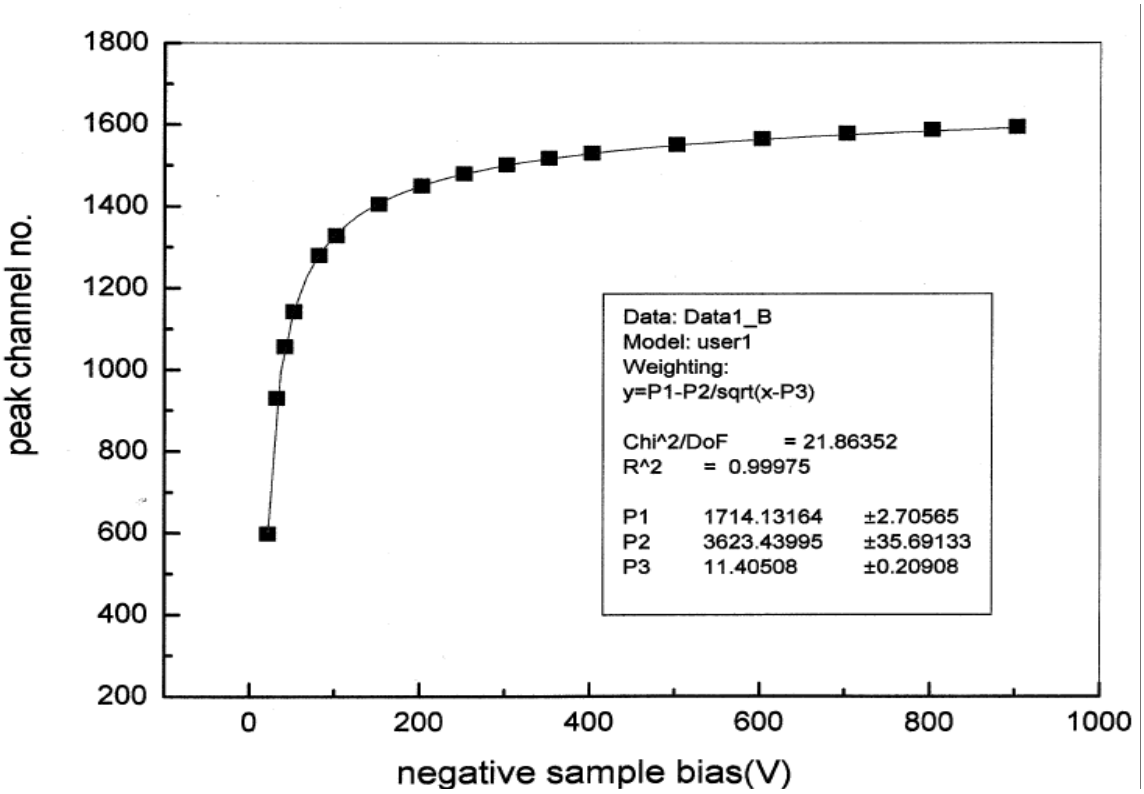

Figure 3.1 Calibration Curve for 6H-SiC

Figure3.2 shows the PAES spectrum obtained from the SiC sample after annealing at 100°C and 950°C. Peaks ascribed to Si, C and O may be seen at ~78 eV,

260 eV and at 500eV respectively. The energy 78 eV corresponds to that the energy of the Si LVV previously observed using EAES for a SiO_2 sample [24]. As can be seen, annealing at 950°C shows the Si LVV peak while the one at 100°C doesn't show one.

PAES spectra of SiC were earlier studied by Nangia et al[25].They used a trochoidal energy analyzer which was not able to resolve the high energy Auger electrons from C and O.

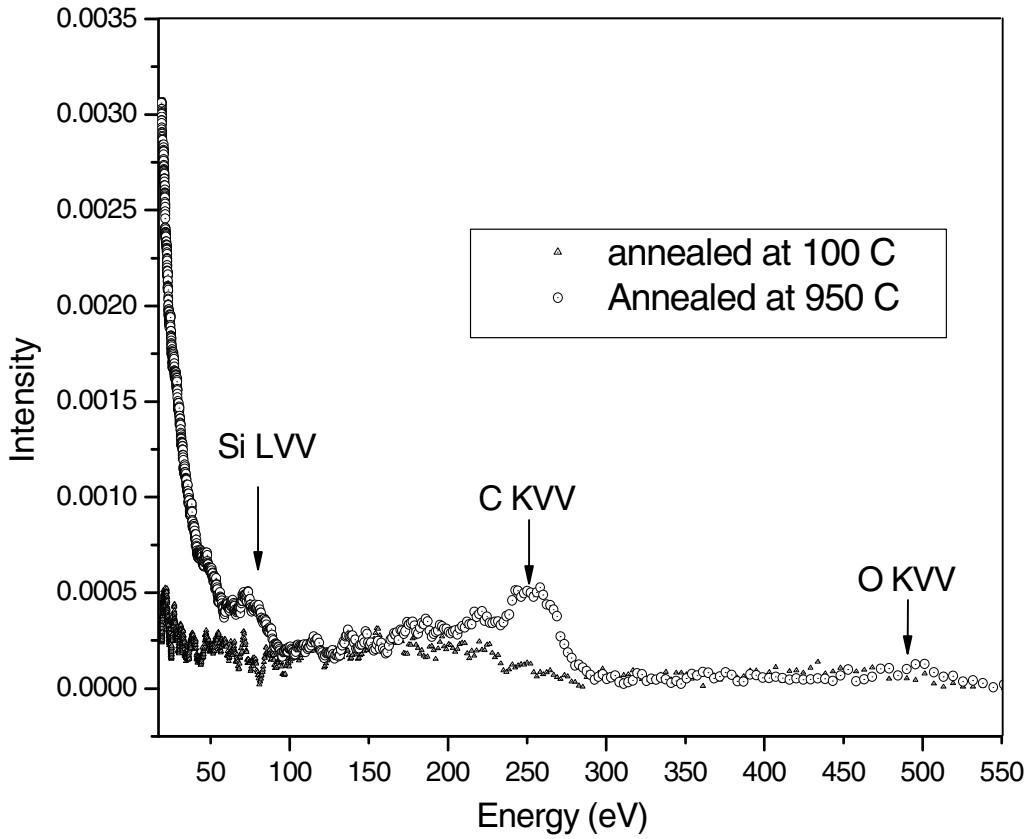

Figure.3.2 TOF-PAES spectrum of SiC taken after annealing at 100°C and 950° C

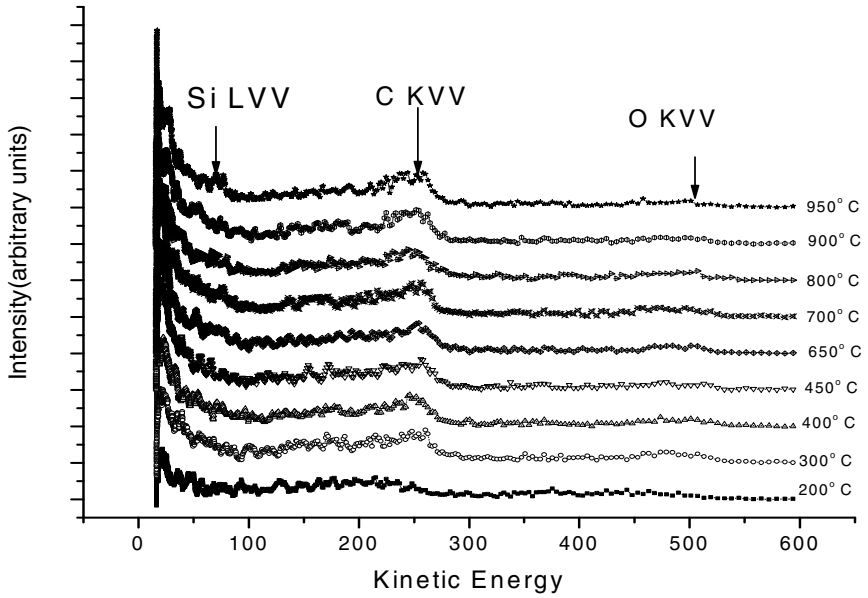

Figure 3.3 TOF- PAES Spectrum of SiC at different annealing temperature

A series of PAES spectra taken after different annealing temperatures are shown in Fig 3.3. The as received sample surface showed little signal in the spectral region of Si and C and large increase in Si and C signal upon vacuum annealing indicates that that surface was initially covered by oxygen which is removed by annealing at 300^{o}C. This change is observed by plotting the percent change in the integrated peak intensity of different elements and is shown in figure 3.4. As can be seen, surface concentration of Si and C increase with increasing temperature. The percent decrease in oxygen is not as significant as percent increase Si or C. The Si intensity increases after annealing at 300^{o}C which is an indication of the surface being cleaned. The increase in Si Signal at 900^{o}C is not consistent with surface graphitization.

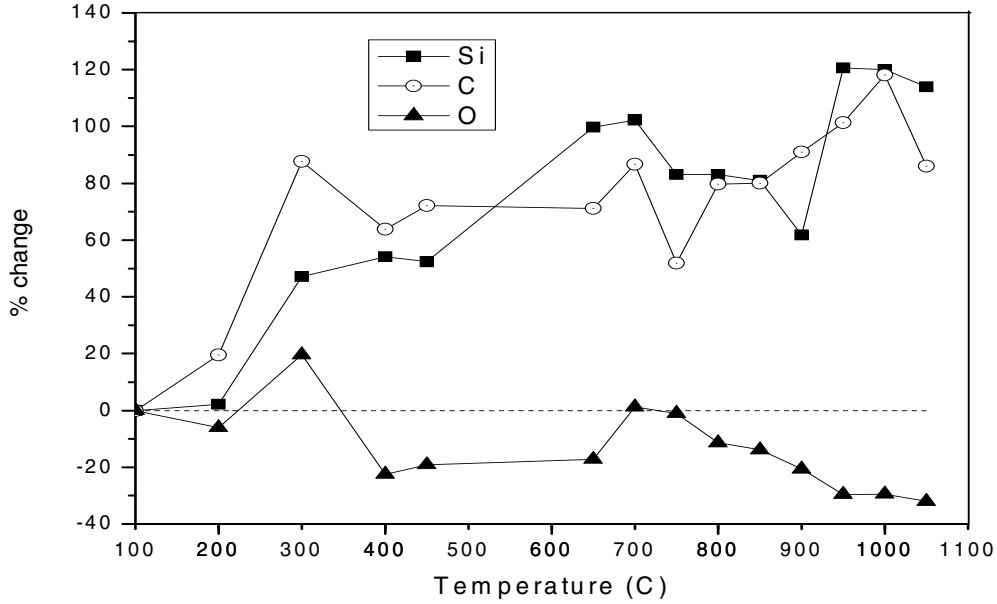

Figure 3.4 Percentage change in intensity of Si, C and O with different annealing temperature

The study of SiC was done to monitor the surface changes in various annealing conditions and to determine its suitability as a moderator. We know that 6H-SiC

Note that the Si and C signals are increasing together with annealing temperature indicating that the surface stoichiometry is not altered with annealing. The knowledge of the surface modification is very important for SiC to be used as a moderator and in Application of SiC composites in Nuclear Fusion reactors and fuel cell/turbine hybrid systems.

The data shown in Fig 3.5 indicates the existence of low energy Auger peaks in SiC. Such peak have ,to our knowledge ,have not been observed earlier presumably due to the difficulty in observing them in conventional Auger or XPS.

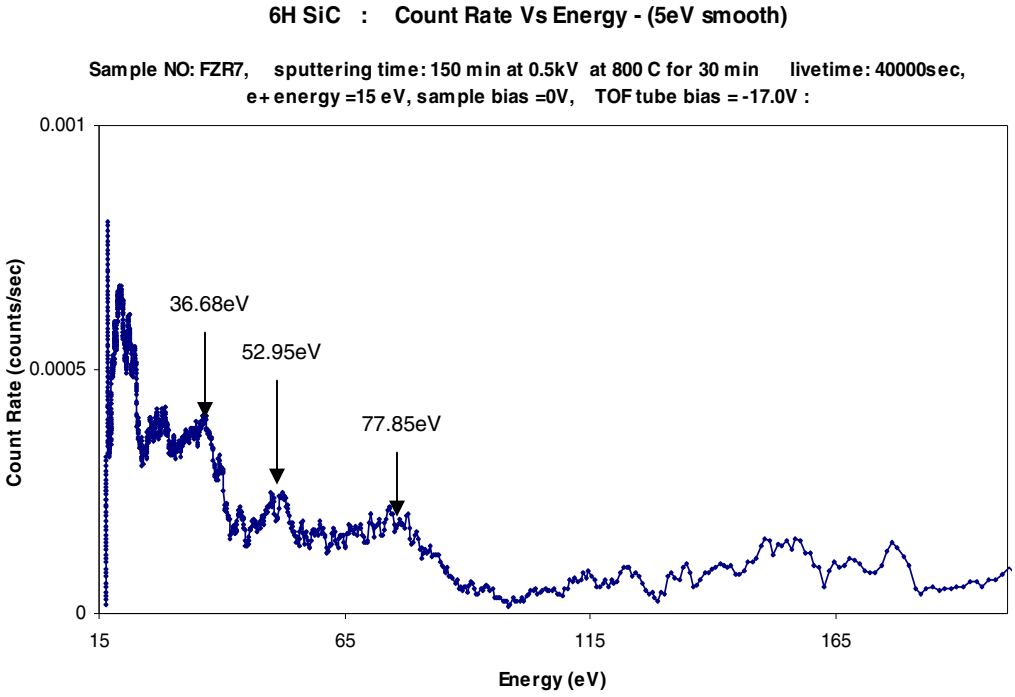

Figure 3.5 TOF –PAES spectrum showing the Low Energy Auger Transitions in SiC

Earlier studies of TOF-PAES have been mostly to measure the Auger peaks at energy >60eV.[20] To verify that the TOF-PAES system works for the low energy Auger electrons, we studied polycrystalline Gold foil (Alfa Aesar, 99.99% purity). Au has several Auger transitions in the low energy range (38eV, 52eV, 67eV and 95eV) and that makes it ideal to study the behavior of the TOF-PAES system in the low energy range.

3.2 TOF-PAES study of Gold

We report the first TOF-PAES study of the Au surface. Figures 3.6-3.9 show the calibration curves for different TOF tube voltage.

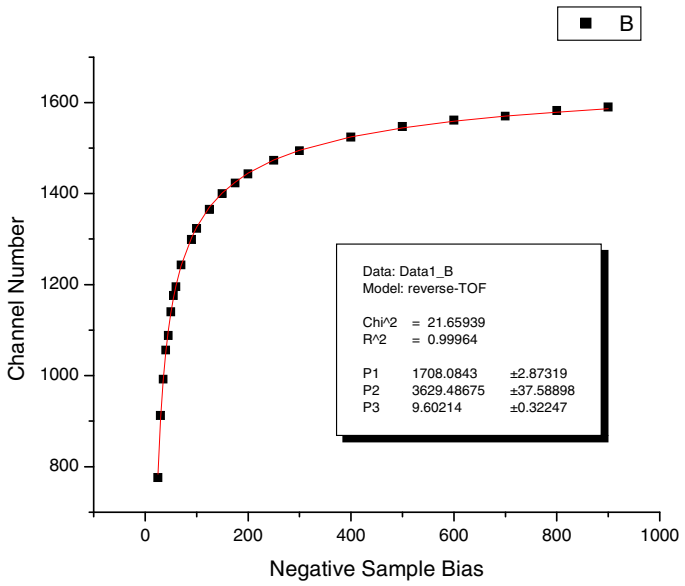

Figure 3.6 Calibration Curve for TOF Tube Voltage=-13V, TAC range=800ns ,Delay=700 ns

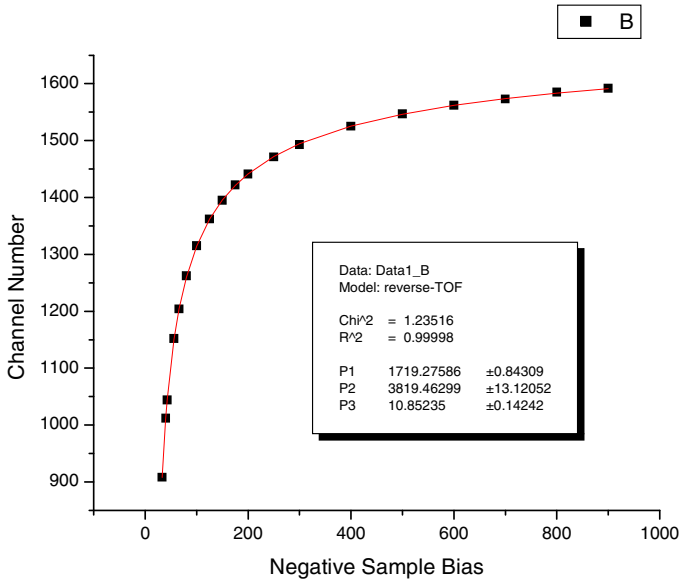

Figure 3.7 Calibration Curve for TOF Tube Voltage=-17V, TAC range=800ns, Delay= 700 ns

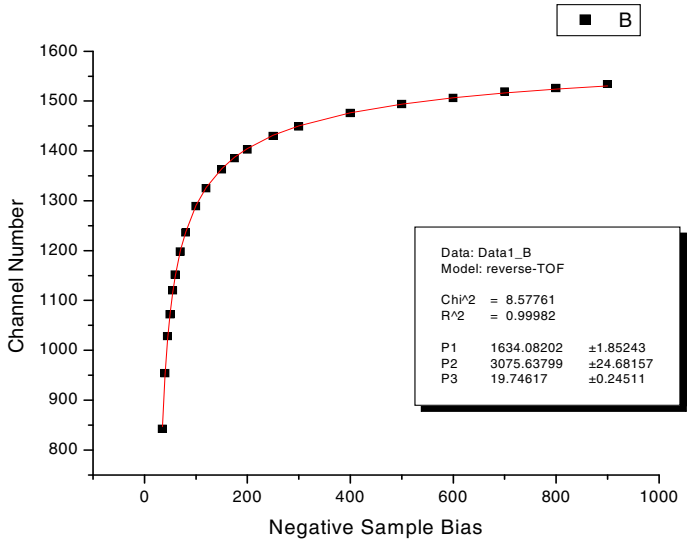

Figure 3.8. Calibration Curve for TOF Tube Voltage=-25V, TAC range=2000ns,Delay= 1500 ns

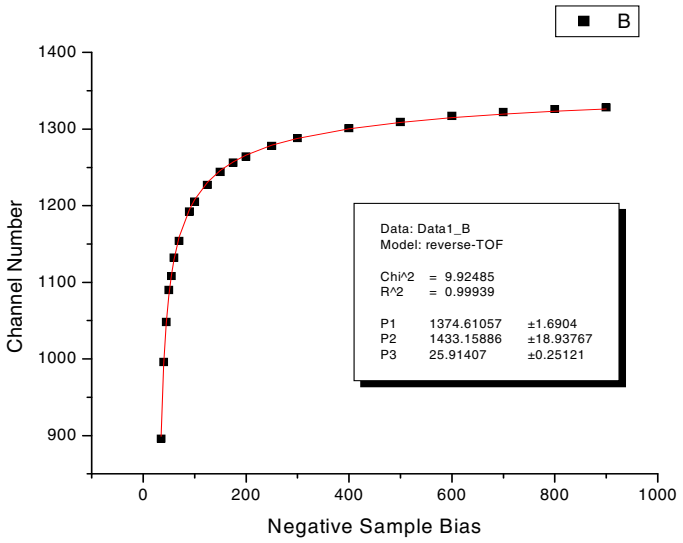

Figure 3.9 Calibration Curve for TOF Tube Voltage=-30V, TAC range=2000ns,Delay= 1500 ns

From these calibration curves we found out the values of the parameters P1, P2 and P3 with varying TOF

Table 3.1 Values of various parameters for different TOF Tube Voltage.

TOF Tube Volt(V)	P1	P2	P3
-13	1708.0843	3629.487	9.60214
-17	1719.27586	3819.46299	10.85235
-25	1634.08202	3075.638	19.74617
-30	1374.61057	1433.15886	25.91407

TOF-PAES spectrum of Au is shown in fig. 3.10. The spectrum was obtained with Time of Flight Tube (TOF Tube) bias set at -17V. The different peaks observed in fig 3.10 are 37.55eV, 52.3eV, 67.54eV and 97.08eV and they correspond to $O_{23}VV$, $N_{67}VV$,O_2VV

and O_1VV transitions respectively. The different Auger peaks and their respective energies are shown in Table 3.2

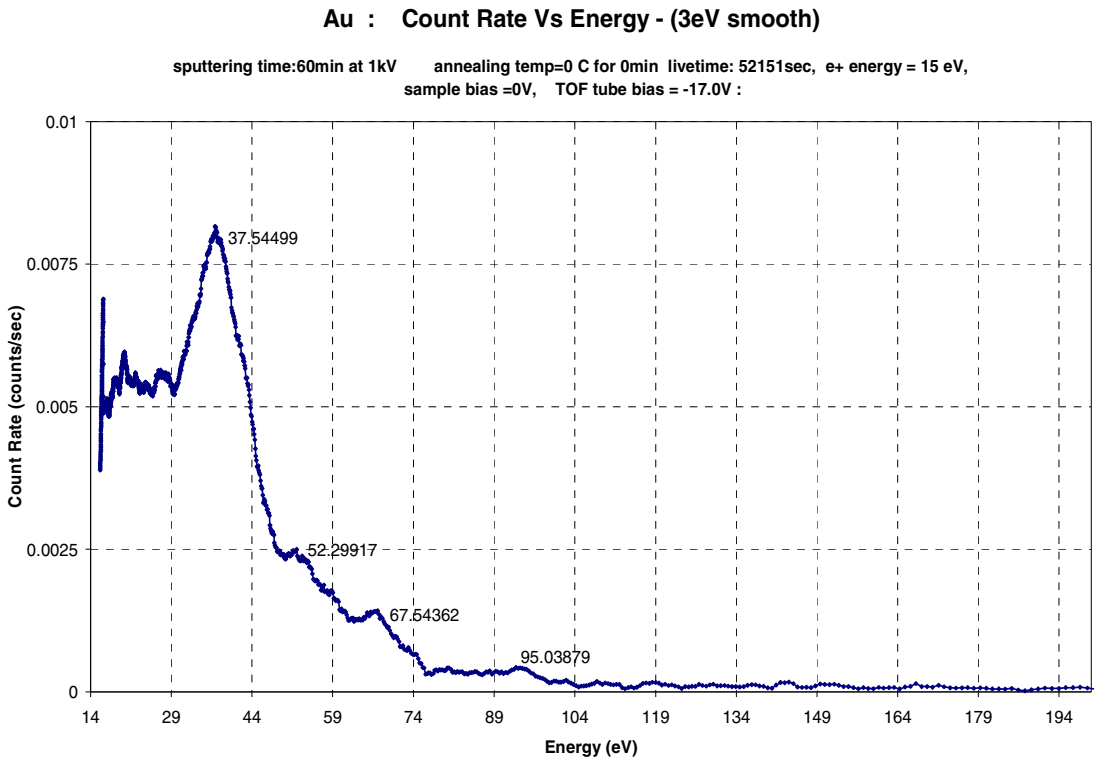

Figure 3.10 PAES spectrum of sputtered Au surface showing different Auger Peaks (TOF Tube Voltage= -17V)

Table 3.2 Different Auger transitions as observed by TOF-PAES

Transition	$O_{23}VV$	$N_{67}VV$	O_2VV	O_1VV
Energy	37.55eV	52.3eV	67.54eV	97.08eV

Figure 3.11, 3.12 and 3.13 show the different spectra of Au with changing TOF Tube bias. As can be see, when the TOF Tube bias is increased (fig 3.12 and fig 3.13) the intensity of the 37.55eV peak decreases. This can be explained by noting that the

electrons with energy closer or less then the TOF Tube bias loose most of their energy while passing through the TOF Tube. Hence the resolution of TOF-PAES is determined, to some extent, by the TOF Tube bias. We have earlier studied Au using PAES.[26] Due to low resolution of the instrument only the 44eV and 97.08 eV peaks are visible. Hence this is the first spectra showing the four low energy Auger transitions in Au.

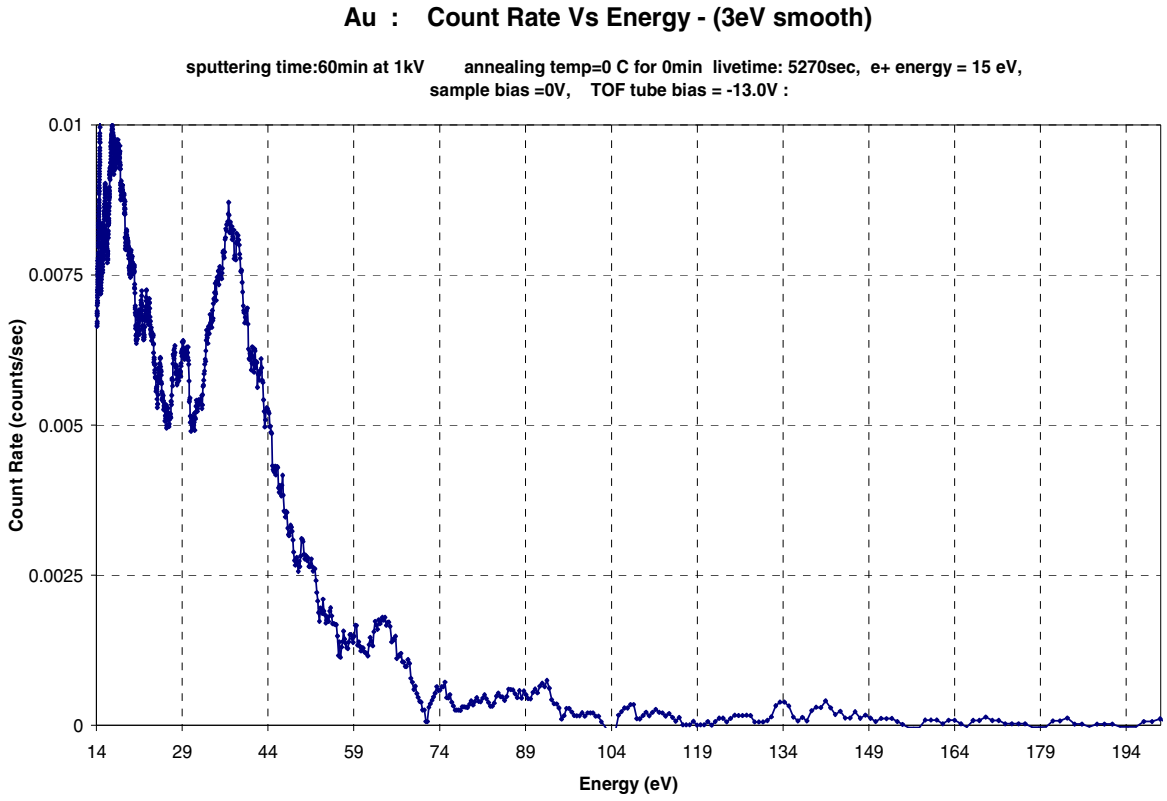

Figure 3.11 PAES spectrum of sputtered Au surface showing different Auger Peaks (TOF Tube Voltage=-13V)

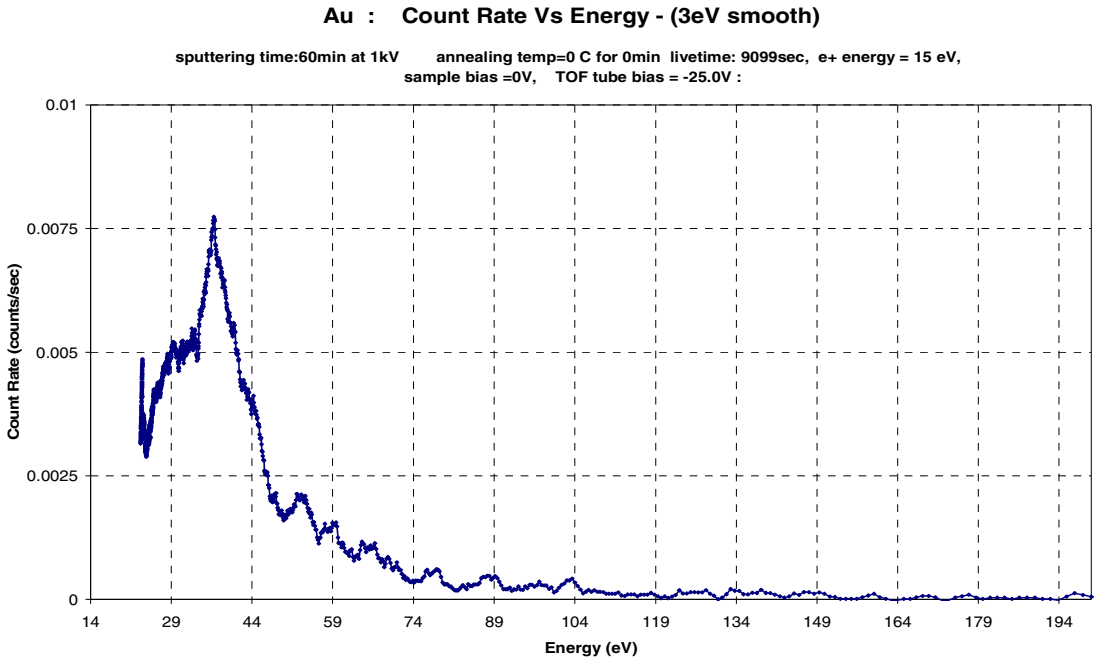

Figure 3.12 PAES spectrum of sputtered Au surface showing different Auger Peaks (TOF Tube Voltage=-25V)

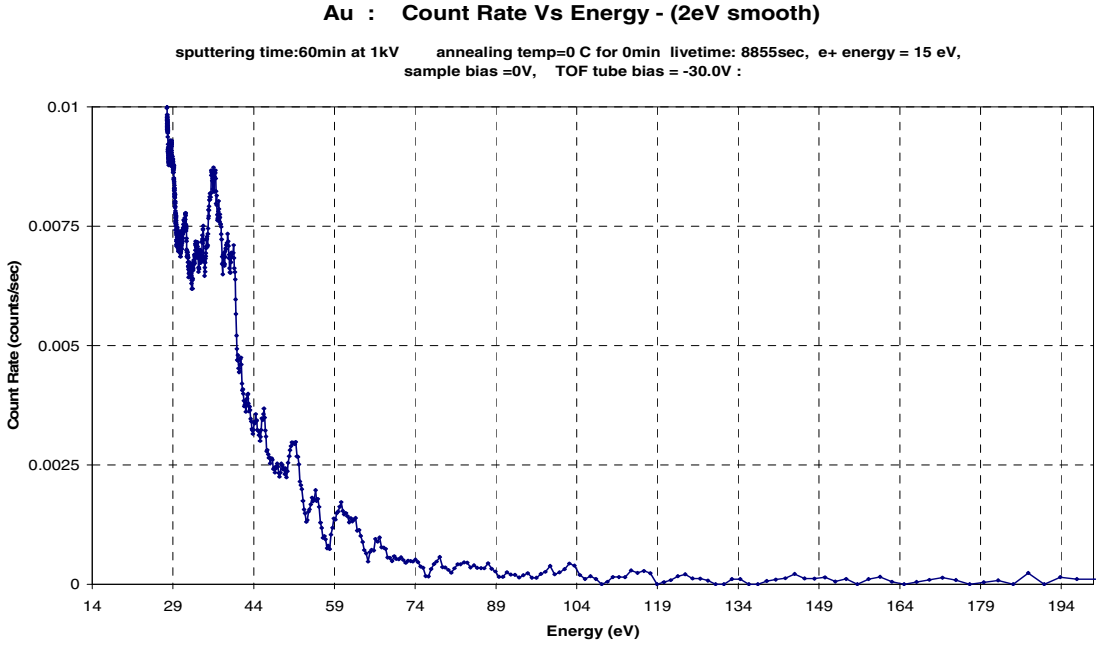

Figure 3.13 PAES spectrum of sputtered Au surface showing different Auger Peaks (TOF Tube Voltage=-30V)

3.2.1 Comparison of the relative experimental intensity to the theoretical intensity

The area under the four different peaks observed in 3.10 was calculated. The $O_{23}VV$ and O_2VV peaks are due to annihilation of positron with the 5p core electron of Au. Hence the sum of their peak integrals must be proportional to the annihilation probability of positron with the 5p electrons. Similarly $N_{67}VV$ and O_1VV peak integrals are proportional to the annihilation probability of positron with the 4f electrons and 5s electrons in Au. Hence the relative positron annihilation was calculated by normalizing the peak integrals to that of $N_{67}VV$ (proportional to positron annihilation probability with 4f core electron in Au). Table 3.3 shows the comparison of the relative positron annihilation probability with the Au core electrons and comparison to the theoretical values.

Table 3.3 Comparison of the relative positron annihilation probability with the Au core electrons and comparison to the theoretical values

	5p($O_{23}VV$+ O_2VV) Normalized to 4f	5s(O_1VV) Normalized to 4f	4f($N_{67}VV$)
Experimental	40.077	0.2862	1
Theoretical[28]	9.96	2.35	1

Major deviation is in the probability for 5s electrons and 5p electron annihilation probability with positron which are experimentally found to be less then that reported in the literature

CHAPTER 4

CONCLUSION

TOF-PAES was applied to measure the elemental contend of the top layer of SiC under various annealing conditions. This work has important implications in determining the suitability of SiC as a positron moderator and in application of SiC composites in Nuclear Fusion reactors and fuel cell/turbine hybrid systems.

We have characterized the 6H-SiC surface using TOF-PAES with different annealing temperature. Si and C signals are increasing together with annealing temperature indicating that the surface stoichiometry is not altered with annealing. There is a jump in Si and C signal ratios at 300^{o}C which can be taken as the temperature at which contaminants begin to desorb from the 6H-SiC surface.

We measured for the first time the relative PAES intensities of Si , C and O from a SiC surface. The TOF-PAES spectrum of SiC also revealed low Energy Auger peaks that are difficult or impossible to observe using convention Auger or XPS due to the large secondary background at low energies. These low energy peaks in SiC change in intensity and energy as compared to Si and this suggests that these peaks are reflective of the state of the Si-C bond in the top most atomic layer.

The ability of PAES to provide information about the elemental content of the top most layers and the bonding state of Si in this layer could be important in providing the

understanding needed to grow epitaxial layers of different polytypes realizing in defect free junctions.

The UTA TOF-PAES spectrometer has been used in new measurements of polycrystalline Au which yielded new information on the annihilation of positrons with 5d, 4f, and 5s core electrons and revealing a partial failure of previous theoretical calculations to account for the correct relative annihilation probabilities. The studies on Gold foil shows the sensitivity of TOF-PAES to Low energy Auger transitions (< 100eV). We also demonstrate, for the first time, simultaneous observation of multiple Low energy Auger transition in Au using TOF-PAES.

REFERENCES

1. H. Morkoç, S. Strite, G.B. Gao, M.E. Lin, B. Sverdlov and M. Burns. J. Appl. Phys. **76** (1994), p. 1363

2. G. Brauer et al ,Applied Surface Science, v 252, n 9, Feb 28, 2006, Proceedings of the Tenth International Workshop on Slow Positron Beam Techniques for Solids and Surfaces SLOPOS-10, p 3342-3351

3. P. A. M.Dirac, 1930, Proc. Cambridge Philos. Soc. 26, p361.

4. Carl D.Anderson, 1932a, *Science* 76, p238.

5. A.R. Koymen , K.H.Lee. G. Yang, K.O. Jensen and A.H. Weiss, Phys.Rev. B, Vol.48, p.2020 (1993)

6. A. Weiss, A. R. Koymen , D. Mehl ,K.H. Lee and G. Yang , Nucl.Ins. and meth., p.591, (1991)

7. A. Weiss, A. R. Koymen , K.H. Lee and Chun Lei , J. Vac. Sci Technol. A., Vol 8, p2517,(1990)

8. A. Weiss, R. Mayer, M. Jibaly, C. Lei, D. Mehl and K. G. Lynn,1988 *Phys. Rev. Lett* 61 p2245

9. K. O. Jensen and A. Weiss, *Phys.Rev. B* 41,3928-3936 (1990)

10. Ed. P. Coleman, Positron beams and Their Applications, p113 (2000)

11. G. Yang, J. H. Kim, S. Yang, A. H. Weiss , 1996, Surf. Sci 367 p45

12. G. Yang, S. Yang, J. H. Kim, K. H. Lee, A. R. Koymen, G. A. Mulhollan and A. H. Weiss, 1994, J. Vac. Sci. Technol. A12 p411.

13. J.H.Kim and A. H. Weiss , 2000 Surf Scie.460 p129.

14. D. Mehl , A. R. Koymen , K.O. Jensen , F. Gotwald and A. H. Weiss,1990 Phys. Rev.B. 41 p799

15. P.J. Schulz and K. G. Lynn , Rev. Mod. Phys., 60 701 (1988)

16. E. Jung ,1996, Ph.D. dissertation (The University of Texas at Arlington)

17. R. Mayer, A. Schwab and A. H. Weiss, 1990 Phys. Rev. B. 41 p3928

18. N. G. Fazleev, J. L. Fry and A. H. Weiss.1998, Phys. Rev.B 57,p12506.

19. N.G. Fazleev, J.L. Fry , J.H.Kaiser, A.R.Koymen, K.H. Lee, T.D. Niedzeiwchi and A.H. Weiss, 1994 Phys.Rev. B 49p10577

20. S.P. Xie, University of Texas at Arlington, Dissertation 2002

21. J. Zhu , University of Texas at Arlington, Dissertation 2004

22. K.F.Canter, P.G. Coleman, T.C. Griffith and G.R. Heyland, 1972, J. Phys.B 5 pl67

23. R. Suzuki, T. Mikado, M.Chiwaki, H. Ohgaki and T. Yamazaki, 1995, Appl. Surf.Sci . 85 p87

24. D.E. Ramaker, J. Vac. Sci. Technol., Vol 16, No.2, (1979)

25. A. Nangia, J.H. Kim, a. H. Weiss, G. Brauer, Journal of Applied Physics, 91,5, (2002), p2818

26.K.H.Lee, A.R. Koymen, D. Mehl ,K. Jensen, A. Weiss ,Surface Science, v 264, n 1-2, Mar 1, 1992, p 127-134

27. K. Oura and T. Hanawa. Surf. Sci. 82 (1979), p. 202

28. P.J. Schultz, K.G.Lynn , Review of Modern Physics,Vol.60,No.3, July 1988,p 701 - 779

BIOGRAPHICAL INFORAMTION

Saurabh Mukherjee received Bachelor of Technology degree in Ceramic Engineering at Banaras Hindu University, India in 2003. After graduation he worked as Ceramic Engineer in Gujarat Glass Ltd. His main responsibilities were improving the performance of high temperature refractory in glass furnace. He started his masters program in Materials Science and Engineering at the University of Texas at Arlington in fall 2004. In spring 2005, he joined the UTA positron surface physics group led by Dr. A.H Weiss in physics department. His research interest is focused on characterization of Silicon Carbide surface using Time of Flight- Positron Annihilation induced Auger Electron Spectroscopy with special focus on determination of TOF-PAES sensitivity to the low energy Auger electrons(<50eV). He wants to continue working on Positron spectroscopy in the same group.